JOURNAL OF MATERIALS SCIENCE **34** (1999) 3327–3333

Observation of salt impurities in ultra-high-molecular-weight polyethylene (UHMWPE)

J. LOOS
Eindhoven Polymer Laboratories, The Dutch Polymer Institute, P. O. Box 513, 5600 MB Eindhoven, The Netherlands
E-mail: j.loos@chem.tue.nl

M. A. WIMMER
AO/ASIF Research Institute, Clavadelerstrasse, 7270 Davos, Switzerland
E-mail: markus.wimmer@ao-asif.ch

Different direct molded ultra-high-molecular-weight polyethylene (UHMWPE) samples have been investigated using reflective light microscopy and scanning electron microscope techniques (low voltage and variable pressure SEM). On the surfaces as well as throughout the material a—to the best of our knowledge—unknown type of impurities has been identified. X-ray element analysis (EDX) was used to characterise these impurities as sodium chloride and potassium chloride salt inclusions.

1. Introduction

Ultra-high-molecular-weight polyethylene (UHMW PE) is a high-density polyethylene with a molecular weight of above 3×10^6 according to ASTM D 4020. Some of the advantageous properties of UHMWPE are the abrasion resistance greater than that of any other thermoplastic material, and a low coefficient of surface friction [1, 2]; the highest impact toughness of any plastic, even at low temperature; good corrosion and chemical resistance; resistance to cyclic fatigue; and resistance to radiation [3].

Preferred applications of UHMWPE are in chemical processing, the food and beverage industries, the lumber industry, medical implants [4], strong and light fibers [5], textiles, transportation and highly efficient battery separators [6].

Currently, UHMWPE is the material of choice in many technical as well as medical applications. However, in spite of its advantageous properties, UHMWPE failure due to wear is of growing concern. Especially, in medical applications, where UHMWPE is used as a bearing material for total knee and hip arthroplasty, particle release from the bulk UHMWPE is considered as a major problem [7–10]. It has been reported that polyethylene debris causes periprosthetic bone resorption (osteolysis) and leads to loosening and, thus, failure of the artifical joint. Hence, considerable attention has been focused on the intrinsic wear properties of UHMWPE.

Under several factors influencing the wear properties of UHMWPE, inclusions are reported to play a crucial role in the failure scenario. Particularly, for abrasion resistance the quantity of extraneous particles or inherent inclusions should be the lowest possible. According to ASTM F 648-84 a 300-gram sample of powder is restricted to no more than twenty-five extraneous particles for medical applications and DIN 58834 suggests upper limits of foreign elements as for titanium, aluminum, calcium and chlorine (20, 40, 50, and 20 ppm, respectively). In this study we report a previously unknown and unexpected type of impurity in UHMWPE compression molded sheets.

2. Experimental

Test sheets of different UHMWPE materials were kindly supplied by Hoechst/Ticona (GUR 1020 and GUR 1120), Germany, Hoechst/Celanese (GUR 4150, PolyHi Solidur Reference UHMWPE), USA, DSM (UH 210 and UH 410), The Netherlands, and Phillips Petroleum Company (non-commercial sample), USA. The test sheets were directly molded using the raw powders without additives. From these sheets samples were cut with a razor blade for reflective light microscopy (LM) and scanning electron microscopy (SEM). All investigations were performed on the untreated surface of the test sheets. In addition, thin microtome cross-sections were prepared for analyses of the bulk morphology.

Reflective light microscopy was carried out using a Zeiss Universal light microscope equipped with crossed polarisers. The micro-features of the samples were examined using a S-4500 Hitachi low voltage SEM (1 kV accelerating voltage, secondary electron detector) and a S-3200N Hitachi variable pressure SEM (20 kV accelerating voltage, 70 Pa pressure, back scattered electron

detector). Both systems were equipped with an Oxford Link Pentafet EDX detector for energy dispersive X-ray spectroscopy. Also this part of the analysis was performed without additional surface treatment or coating. A survey of low voltage SEM applications on polymers is given in [11, 12].

3. Results and discussion

The surfaces of all investigated samples showed identical defects: scratches of different length, pitting and embedded particles. A representative example of the surface of one of the molded sheets is shown in Fig. 1. Scratches and standard roughness of technical mold are replicated on the polyethylene surface which explains the imperfect appearance of the test sheets. The adhesive wall/sheet interaction is responsible for pitting. Beside these defects third body inclusions or embedded particles are visible on the surface of the test sheets.

The authors will focus their interest on a special type of these impurities, marked with arrows in Fig. 1 and shown in Fig. 2 at higher magnification, and named as salt impurity (SI). The typical appearance of this type of impurity is an agglomeration of cube-like, or dendritic particles embedded in a circular matrix, independent of the powder type used for the sheet preparation. Adjusting the plane of focus of the light microscope at different height levels the SI seemed to sit on the surfaces of the

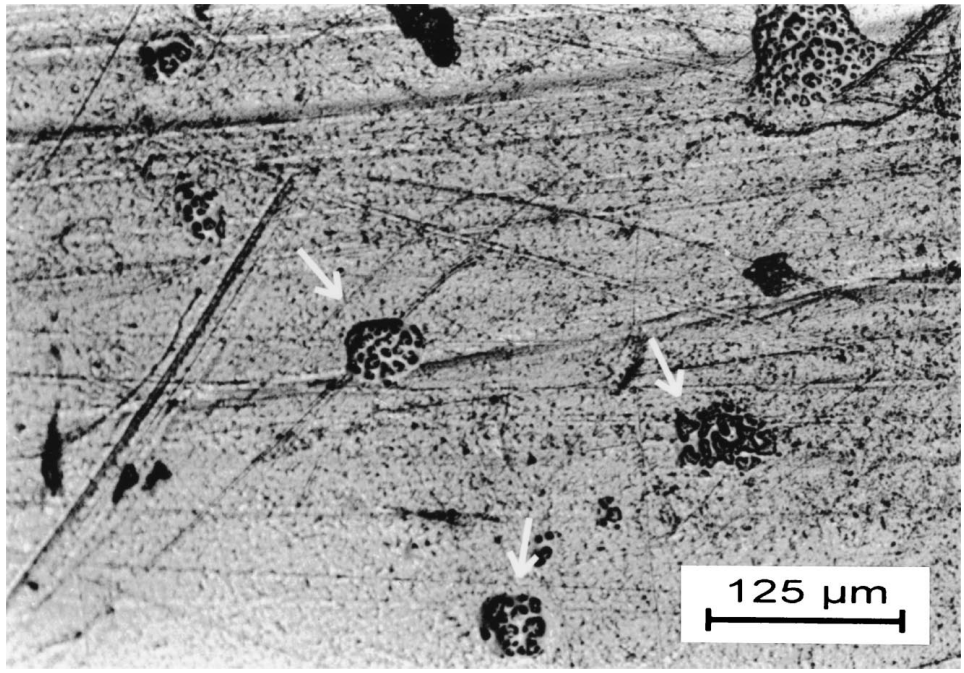

Figure 1 Reflective light microscope image of the surface of a direct molded test sheet (GUR 1020). Impurities under investigation are marked with arrows.

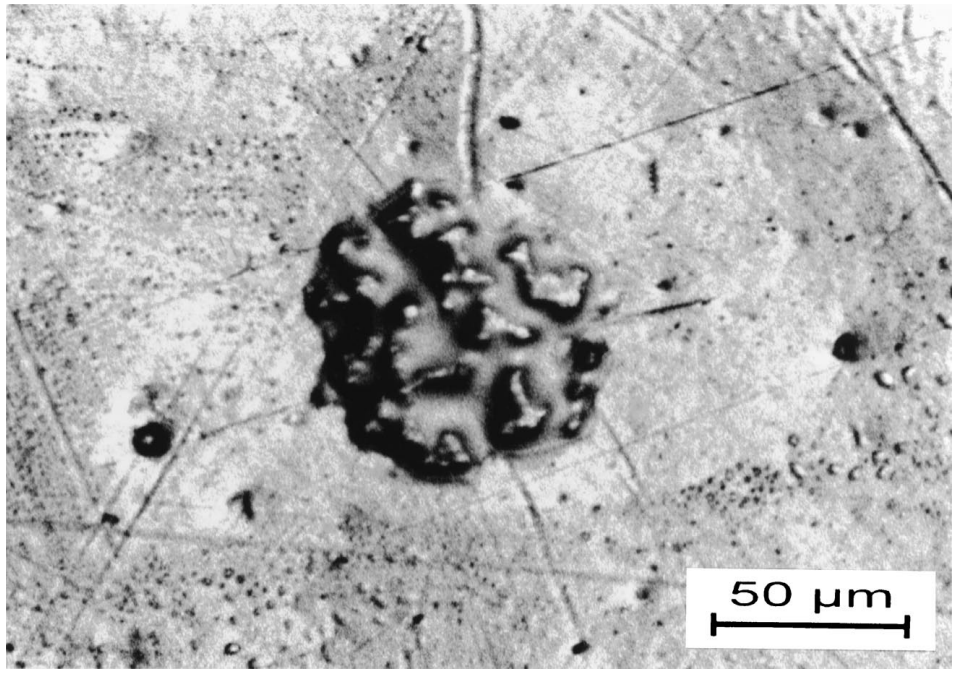

Figure 2 High magnification reflective light microscope image of a salt impurity (SI) formed by dendritic particles. Note the embedding in a circular matrix.

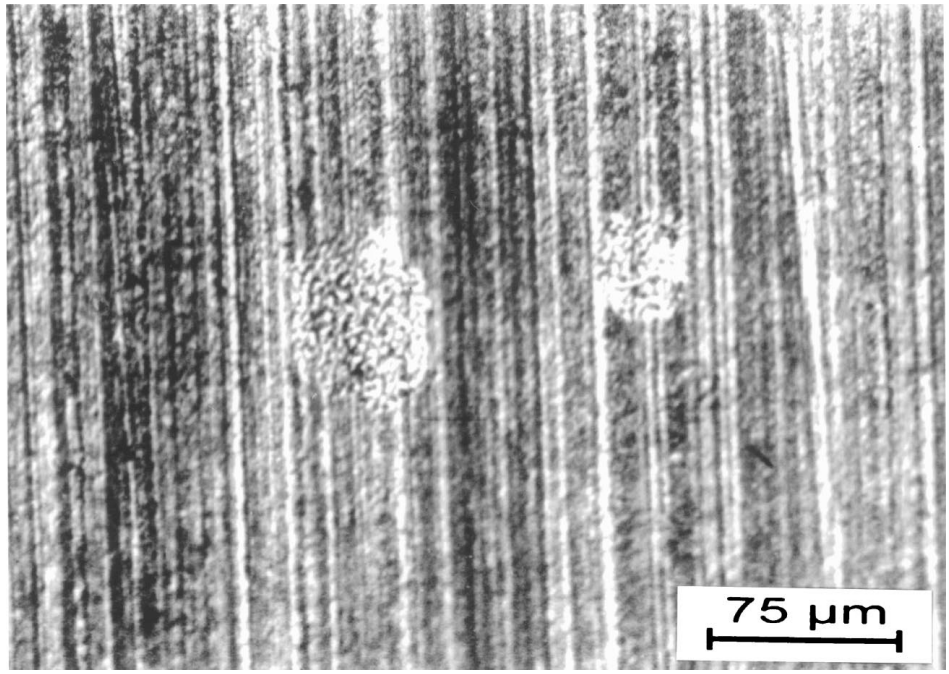

a)

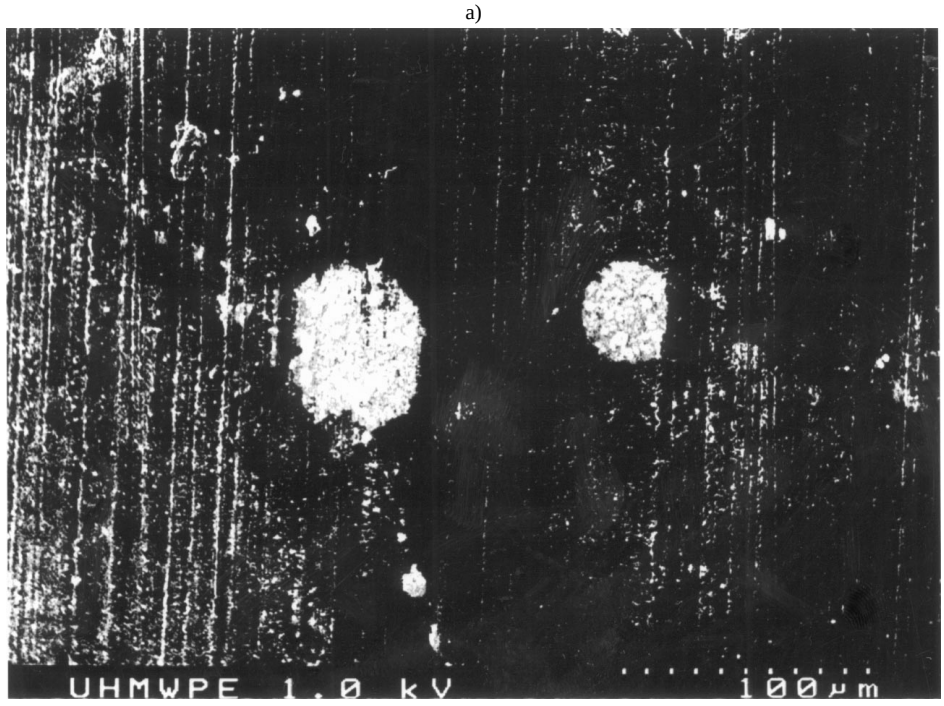

b)

Figure 3 (a) Reflective light microscope and (b) low voltage SEM images of thin microtome cross-sections (UH 210).

test sheet and may be caused by excremention during the molding process.

Fig. 3a represents a reflective light microscope image of a cross-sectioned test sheet. The vertical striations indicate the cutting direction and result from defects of the knife blade of the microtome. In the center of the image two SI are visible with diameters of approximately 30 and 50 μm. In addition to the circular shape of the entire impurity, its individual cubic-like particles can be differentiated from each other. To collect further information the identical sample area as in Fig. 3a was investigated using low voltage SEM (Fig. 3b). The low acceleration voltage of 1 kV results in low penetration depth of the primary electron beam in the sample, and the secondary electron image represents the surface topography. The particles are well defined and embedded in the matrix material. Because the shape of the matrix appears circular on a two-dimensional cross-sectional image, it is suggested that the original three-dimensional shape of the SI is spherical.

More details about the SI composition can be resolved using variable pressure SEM (Fig. 4a). A SEM chamber pressure of 70 Pa and an acceleration voltage of 20 kV is sufficient to perform X-ray element analysis (EDX). At the same time a satisfactory number of backscattered-electrons (BSE) are generated which can be used to produce images without charging artefacts of the non-conductive sample. The accelerating voltage of 20 kV results in a longer penetration path of the primary electrons in the sample and in a high

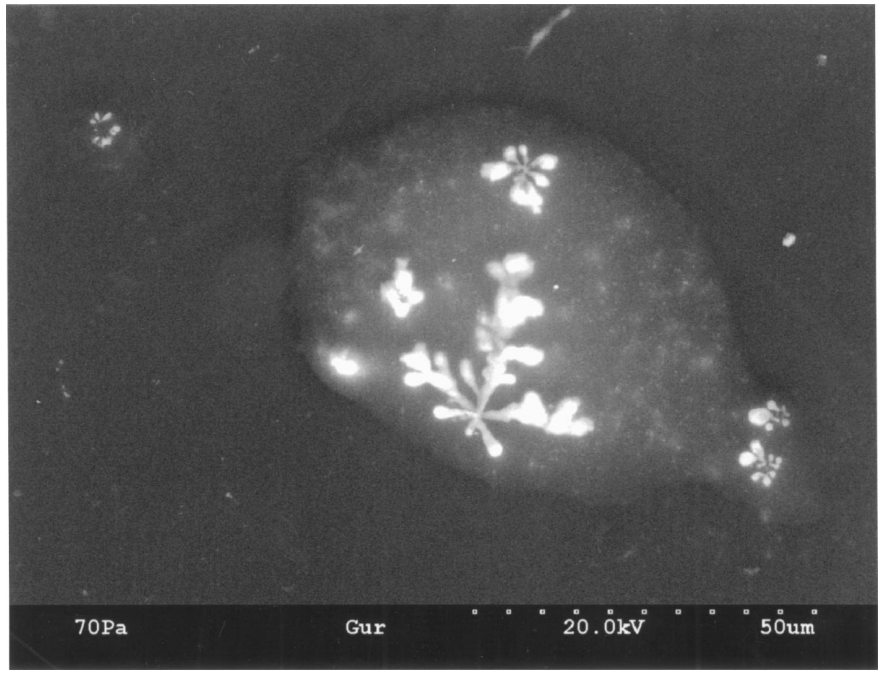

a)

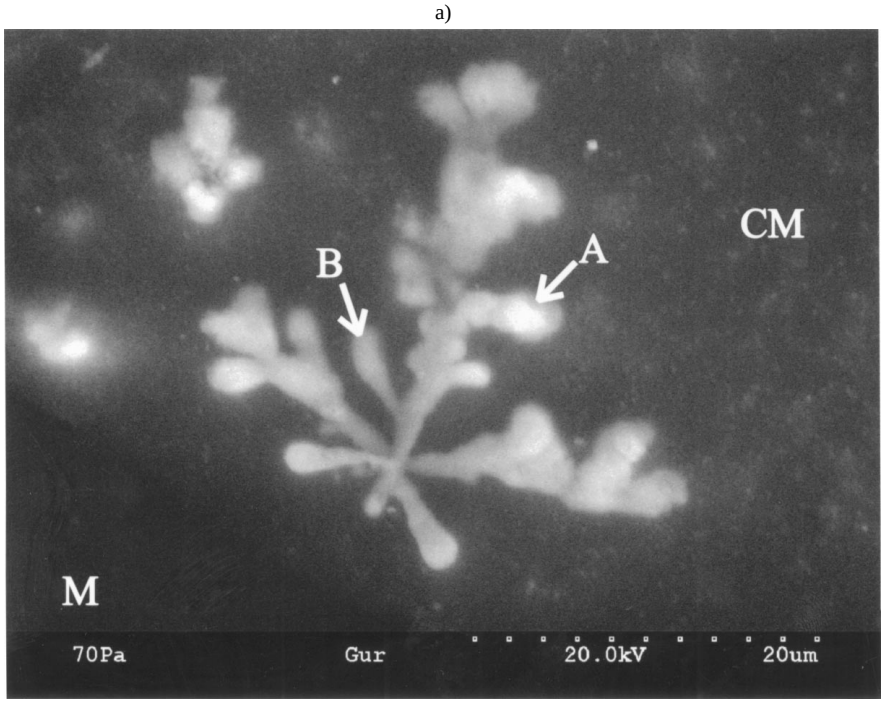

b)

Figure 4 (a) Variable pressure SEM image of a test sheet surface (GUR 1020) and (b) high magnification of one dendritic particle. Areas for EDX-point analyses are indicated as **M, CM, A** and **B.**

yield of BSE. Detection of these electrons with a special detector leads to an increased information depth and to high materials contrast. The contrast is based on different backscattered-electron coefficients dependent on the atomic number of the investigated element [13]. Therefore, the brightness variations in Fig. 4a reflect sample areas with different materials composition: the UHMWPE surrounding appears dark, the cube-like and dendritic particles are bright—indicating a higher atomic number—and the circular matrix looks brighter than UHMWPE.

Further details of the SI composition can be evaluated at higher magnification (Fig. 4b). The dendritic particles do not have a constant brightness at all locations, but rather show BSE-contrast variations. The latter may result from differences in the interaction depth of the backscattered electrons, such as the BSE-signal from the subsurface returns weaker and less intense than the signal from the surface. Another possibility may be due to differences in the SI element compositions. To clarify the reasons of the intensity variations we used the identical sample area for EDX. According to other reports of defects found in UHMWPE devices [14–16], most impurities are composed of minerals (e.g. calcium, titanium, aluminum, and silicon), which are part of the catalyst system, or consist of known additives. The latter are for example calcium stearates, which minimize

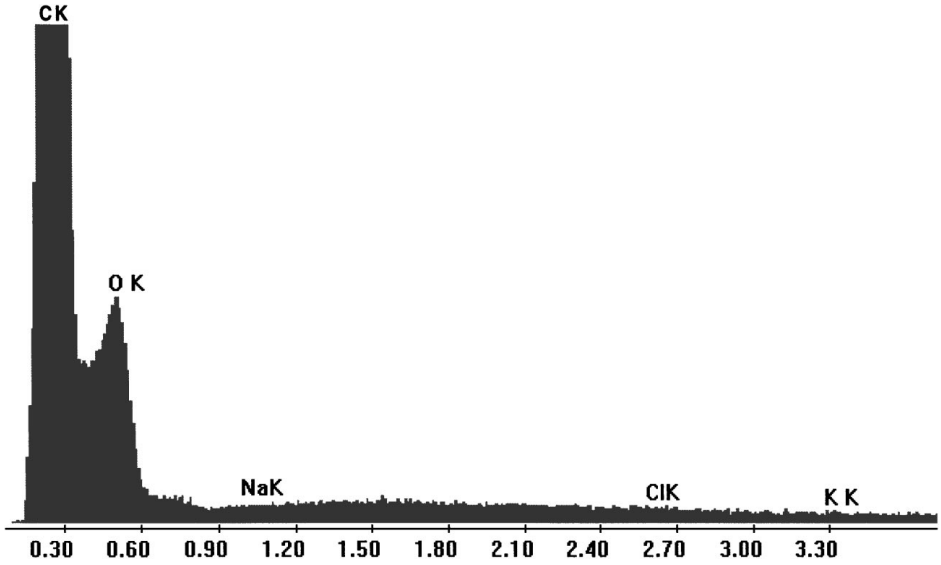

a)

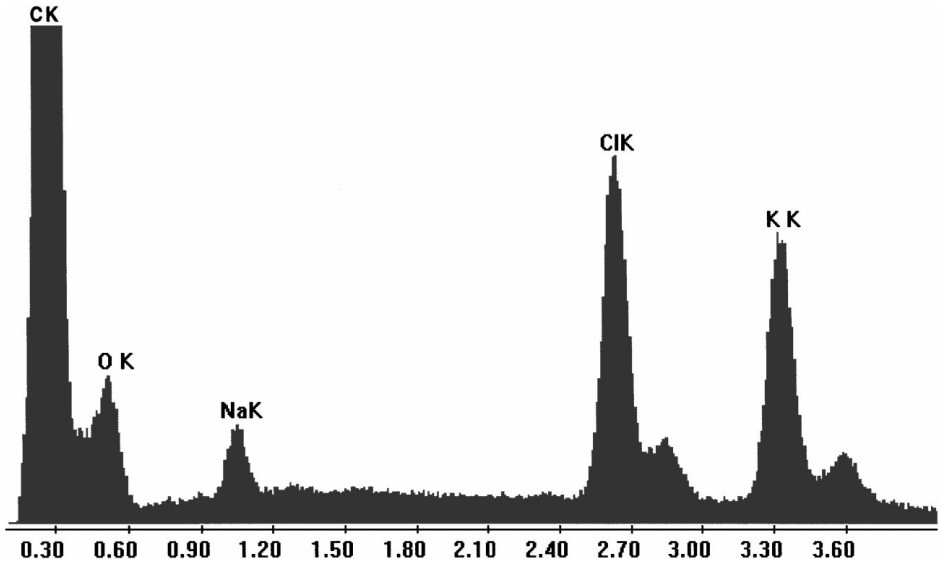

b)

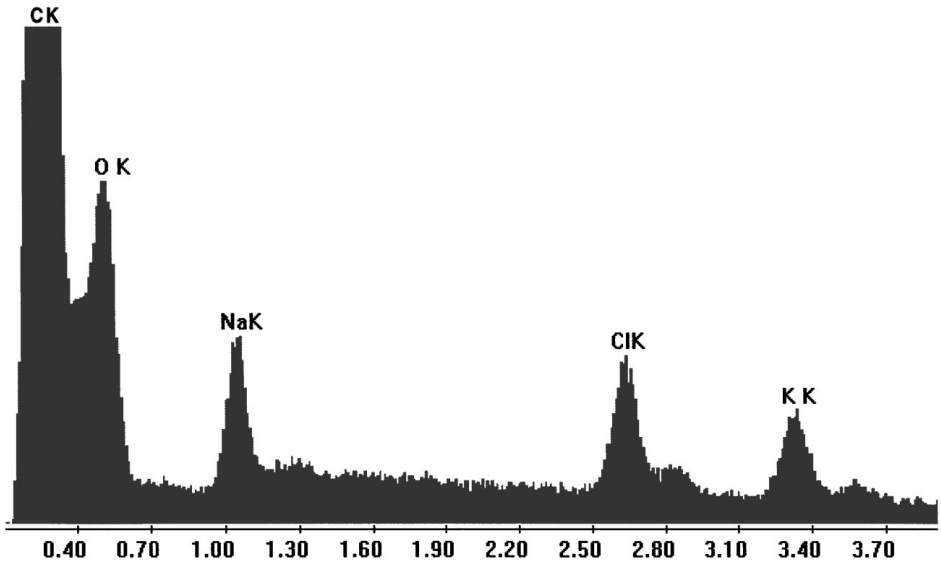

c)

Figure 5 EDX-point analyses of areas indicated in Fig. 4b: (a) UHMWPE (**M**); (b) bright area of the inclusion (**A**); (c) greyish area of the inclusion (**B**); and (d) circular shaped matrix (**CM**); intensities in a.u. and energies in keV. (*Continued*.)

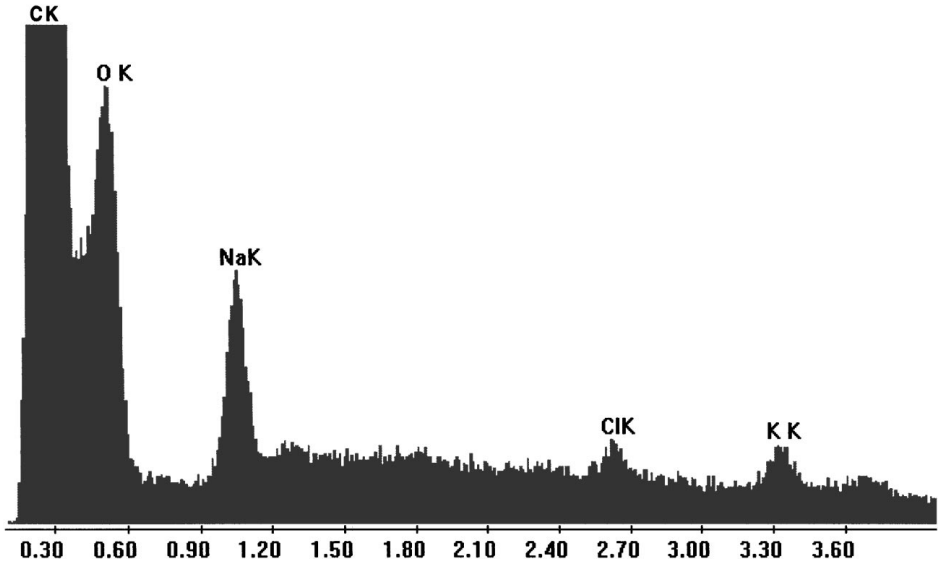

d)

Figure 5 (*Continued*.)

yellowing of the material during various methods of fabrication and increases the processibility of the raw powder. Fig. 5 displays the EDX plots of several regions of the SI using the variable pressure SEM technique. For comparison the element composition of the pure UHMWPE matrix (**M**) is reflected in Fig. 5a. The peaks at approximately 0.3 and 0.5 keV can be determined as carbon and oxygen. The occurrence of oxygen indicates surface oxidation, and because of the high intensity the top of the carbon peak is cut for visualization reasons in all plots of Fig. 5.

The penetration depth of the primary beam results in a large interaction volume due to the high acceleration voltage of 20 kV used. Therefore carbon and oxygen peaks appear in every of the following plots. Fig. 5b shows a point analysis of the bright area, labelled with **A** in Fig. 4b. In addition to carbon and oxygen, peaks at energy levels of approximately 1.1, 2.6, 2.8, 3.3 and 3.6 keV are visible and are determined to sodium (Na-K), chlorine (Cl-Kα and Cl-Kβ) and potassium (K-Kα and K-Kβ), with high intensities of chlorine and potassium. As shown in Fig. 5c, the relative quantity of these three elements changes when darker region of the impurity are analyzed (see label **B** in Fig. 4b). While the sodium intensity remains constant (using the oxygen peak as an internal standard), the intensities of chlorine and potassium are reduced. The investigation of the circular shaped impurity matrix (label **CM**, Fig. 4b) resulted in the same sodium intensity but in a less intense signal of chlorine and potassium (Fig. 5d). Further X-ray analyses of the SI in cross-sectioned samples resulted in the same element composition and element distribution as for the surface impurities.

4. Conclusion

Low voltage SEM proofed to be a powerful technique for the investigation of untreated polyethylene samples. In particular, an up to now unknown type of impurity has been identified and determined to consist of sodium, potassium and chlorine. While the elemental composition was identical for all detected impurities—independent of test sheet and investigated area—, the elemental distribution varied on location inside each impurity. Based on the elemental findings it is suggested that the cube-like, dendritic particles reflect salt minerals which are harder than the polyethylene matrix. The presence of these hard particles raises concerns about the wear properties of directly molded UHMWPE components. Again it should be highlighted that the findings were independent of powder type and manufacturer which raises questions about the time of contamination. Further studies are necessary to understand the particular role of salt particles within the wear process of UHMWPE.

Acknowledgements

The authors gratefully thank J. Petermann (University Dortmund, Germany) and E. Schneider (AO/ASIF Research Institute, Switzerland) for remarks and fruitful discussions, and K. Trinckauf (Hitachi Scientific Instruments, Nissei Sangyo GmbH, Germany), who made the variable pressure SEM available.

References

1. H. HOHN and W. MATERNE, *Kunststoffe* **82** (1992) 391.
2. N. FREISLER, *ibid.* **81** (1991) 809.
3. Encyclopedia of Polymer Science and Engineering, 2nd ed. (Wiley-Interscience, New York, 1985) Vol. 6, p. 490.
4. S. LI and A. H. BURSTEIN, *J. Bone and Joint Surg* **76-A** (1994) 1080.
5. Information Brochure, Dyneema, DSM High Performance Fibers B. V., The Netherlands.
6. M. J. WEIGHALL, in "Worldwide Trends in Battery Seperator Technology and Usage," 6th International ILZRO Battery Seminar, Nizza, May 1992.
7. M. A. WIMMER, T. P. ANDRIACCHI, R. N. NATARAJAN, J. LOOS, M. KARLHUBER, J. PETERMANN, E. SCHNEIDER and A. G. ROSENBERG, *J. Arthroplasty* **13** (1998) 8.

8. A. WANG, A. ESSNER, C. STARK and J. H. DUMBLETON, *Biomaterials* **17** (1996) 865.
9. T. P. SCHMALZRIED, P. CAMPBELL, A. K. SCHMITT, I. C. BROWN and H. C. AMSTUTZ, *J. Biomed. Mater. Res. (Appl. Biomater.)* **38** (1997) 203.
10. P. CAMPBELL, S. MA, B. YEOM, H. MCKELLOP, T. P. SCHMALZRIED and H. C. AMSTUTZ, *J. Biomed. Mater. Res.* **29** (1995) 127.
11. E. A. BURKE, *IEEE Trans. Nucl. Sci.* **NS-27** (1980) 1760.
12. J. H. BUTLER, D. C. JOY, G. F. BRADLEY and S. J. KRAUSE, *Polymer* **36** (1995) 1781.
13. J. GOLDSTEIN *et al.*, "Scanning Electron Microscopy and X-ray Microanalysis" (Plenum Press, New York and London, 1992) pp. 92–94.
14. P. EYERER, *Trans. Soc. Biomater.* **8** (1985) 184.
15. M. B. MAYOR, M. WRONA, J. P. COLLIER and R. E. JENSEN, *Trans. Orthop. Res. Soc.* **18** (1993) 292.
16. P. S. WALKER, G. W. BLUNN, A. B. JOSHI and S. SATHASIVAM, *ibid.* **18** (1993) 499.

Received 23 December 1998
and accepted 27 January 1999